Thermochimica Acta, 49 (1981) 247—258
Elsevier Scientific Publishing Company, Amsterdam — Printed in Belgium

THE THERMAL DECOMPOSITION OF BIS(TRISPYRROLIDINO PHOSPHINE OXIDE) TETRANITRATO URANIUM(IV)

M.E. BROWN *

Chemistry Department, Rhodes University, Grahamstown 6140 (South Africa)

C.P.J. VAN VUUREN ** and A. LITTHAUER

Chemistry Department, University of Port Elizabeth, P.O. Box 1600, Port Elizabeth 6000 (South Africa)

(Received 20 April 1981)

ABSTRACT

The thermal properties of $U(NO_3)_4 \cdot 2$ L (L = trispyrrolidino phosphine oxide) have been examined using thermogravimetry, differential scanning calorimetry and evolved gas analysis by repetitive gas chromatography. Decomposition of single crystals begins around 360 K, approximates to

$U(NO_3)_4 \cdot 2\ L(s) \rightarrow UO_2(NO_3)_2 \cdot 2\ L(s) + \text{gases}$

and is strongly exothermic ($\Delta H = -154 \pm 4$ kJ mole^{-1}). The shape of the exotherm is dependent upon sample mass and self-heating which induces melting. Most consistent results were obtained by reducing self-heating by crimping sample pans and using helium as carrier gas. Grinding of the crystals altered the shape of the exotherm and reduced the value of ΔH to -108 ± 6 kJ mole^{-1}. From EGA results it is concluded that the gaseous products contain N_2, N_2O, NO and NO_2 as well as some H_2O and CO_2. It is suggested that the primary decomposition product is NO_2 and that this oxidizes some ligand, L, to produce the H_2O and CO_2 and to form the lower oxides of nitrogen.

The apparent activation energy for the initial stages of decomposition of crystals (360—385 K) was estimated from isothermal DSC curves as 157 ± 5 kJ mole^{-1}. For ground material (<100 mesh) the activation energy (370—395 K) was increased to 185 ± 14 kJ mole^{-1}.

INTRODUCTION

The thermal stability of hexanitrato uranium(IV) complexes of the type $M_2U(NO_3)_6$, where M = NMe_4^+, NEt_4^+ and Cs^+, has been shown [1,2] to be influenced by the nature of the cation, M^+, used to stabilize the uranium(IV). Such complexes are also more stable than the neutral complex $U(NO_3)_4 \cdot 2$ tdpo (where tdpo = tris(dimethylamido)phosphine oxide) which decomposes at room temperature even when stored in the dark. The thermal stability of the neutral complex $U(NO_3)_4 \cdot 2$ trispyrpo (where trispyrpo = tris(pyrrolidino phosphine oxide) resembles that of the hexanitrato species rather than the

* To whom correspondence should be addressed.
** Present address: UCOR, P.O. Box 4587, Pretoria, 0001, South Africa.

0040-6031/81/0000—0000/$02.50

other neutral complexes and this is attributed to the strong donor properties of the trispyrpo ligand towards uranium(IV). It was thus of interest to investigate the thermal decomposition of $U(NO_3)_4 \cdot 2$ trispyrpo.

EXPERIMENTAL

Preparation of $U(NO_3)_4 \cdot 2$ trispyrpo

A solution of 1.00 g of trispyrrolidino phosphine oxide (trispyrpo) in 10 cm^3 CH_2Cl_2 was added to 1.70 g $CsU(NO_3)_6$ under 3 cm^3 of acetone. The mixture was cooled in ice, stirred for 5 min and filtered. Seven cm^3 of acetonitrile was added to the filtrate and this was left to crystallize at 0°C. Large (up to 3 mm) crystals with a cubic habit were obtained. [U(IV) analysis: 23.8 ± 0.1%; calcd. 23.79%.]

Preparation of $UO_2(NO_3)_2 \cdot 2$ trispyrpo

The stoichiometric amount of ligand was dissolved in 10 cm^3 CH_2Cl_2 and added to a solution of $UO_2(NO_3)_2 \cdot 6\ H_2O$ in acetone. Yellow crystals started to form almost immediately. The crystals were filtered, washed with petroleum ether and dried in vacuum. [U(IV) analysis: 26.8%; calcd. 26.62%.]

Thermal analysis

The thermal properties of $U(NO_3)_4 \cdot 2$ L were examined using a Perkin-Elmer thermal analysis system (TGS-2 and DSC-2). The carrier gas from the DSC (both N_2 and He were used in separate studies) could be sampled into a Taylor-Servomex gas chromatograph with matching carrier gas, a thermal conductivity detector (TCD) and a 1.8 m × 1.6 mm inner diameter stainless-steel column, packed with Porapak Q (80—100 mesh). Other packings, namely silica gel and molecular sieve MS 5A, were also used but Porapak Q gave better separations [3], although it cannot separate N_2, O_2, CO and NO at room temperature. A liquid air trap could be interposed between the GC and the DSC to aid in separation and identification of the evolved gases.

RESULTS AND DISCUSSION

Thermal analysis and stoichiometry

Crystals of $U(NO_3)_4 \cdot 2$ L, on heating at 2 K min^{-1} in N_2, begin to decompose above 84°C (357 K). The rate accelerates to explosive decomposition around 90°C (363 K), as can be seen in the TG trace (Fig. 1). Decomposition is strongly exothermic. The shape of the exotherm on the DSC record, at 5 K min^{-1} in N_2, is very dependent upon sample mass and upon the thermal contact of the sample with the container. When the sample mass is relatively large and thermal contact is poor, rapid self-heating occurs, giving sharp exo-

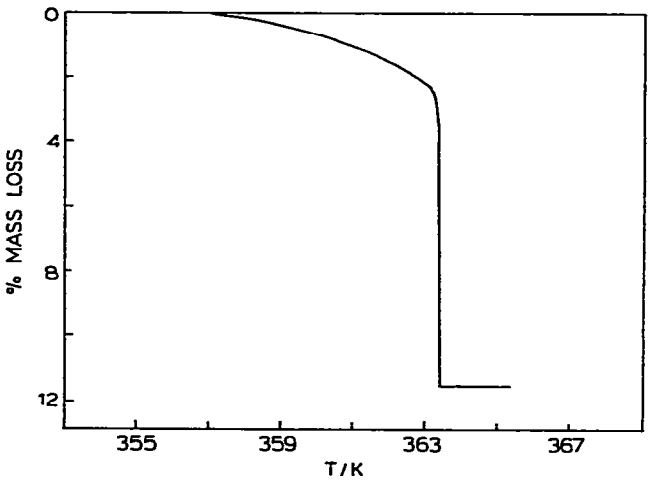

Fig. 1. Thermogravimetry of crystals of $U(NO_3)_4 \cdot 2$ trispyrpo. Heating rate 2 K min^{-1} in N_2.

therms (Fig. 2, curves B and C) and a high overall mass loss (11—12%). The solid residue of such scans shows signs that melting has occurred. On reducing the sample mass, or, for larger sample masses, on crimping the sample pans and thus improving thermal contact, a more symmetrical exotherm is obtained (Fig. 2, curve A) (onset ~365 K, maximum at 380 K and return to baseline ~400 K). The solid product is then pseudomorphic with the reactant, with no marked signs of reaction other than the colour change from green to

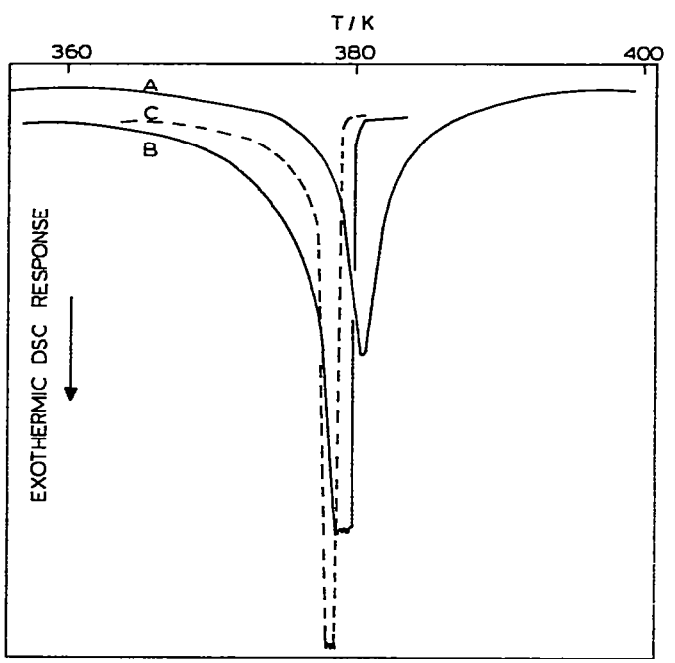

Fig. 2. DSC scans on uncrimped samples of $U(NO_3)_4 \cdot 2$ trispyrpo. Heating rate 5 K min^{-1} in N_2. A, 2.97 mg; B, 4.38 mg; C, 3.30 mg.

brownish-red. Other ways of reducing self-heating effects were to use a very slow heating rate or, most effectively, by using helium, with its high thermal conductivity, as carrier gas. The use of helium also enhances the sensitivity of evolved gas analysis (EGA) (see below), but necessitates re-calibration of the indicated temperatures.

Grinding the crystals to a powder (<100 mesh) has a marked effect on the exothermic DSC response, as shown in Fig. 3. At least two overlapping exotherms are evident in scan A for the ground material. The main exothermic process is shifted to higher temperatures, while the first exotherm is in the same temperature interval as the exotherm for crystals (scan B). Scan B is shown with sensitivity reduced by $X\frac{1}{2}$ and quantitative measurements (see below) confirm that the overall area of the exothermic response is reduced on grinding.

The mass loss calculated for

$$\underset{A}{U(NO_3)_4 \cdot 2\ L(s)} \rightarrow \underset{B}{UO_2(NO_3)_2 \cdot 2\ L(s)} + 2\ NO_2(g) \qquad (1)$$

where $L = (C_4H_8N)_3PO$ is 9.2%. Mass losses close to this value were measured in TG runs at slow heating rates. For runs where self-heating was marked, mass losses of up to 12% were recorded.

The solid decomposition product (compound B) was brownish-red, whereas $UO_2(NO_3)_2 \cdot 2$ L prepared from solution (compound C) is yellow. No U(IV) was detected in compound B. The UV/visible spectra of compounds B and C are similar except for the charge transfer band which occurs at about 500 nm in C. The X-ray powder diffraction patterns of B and C are considerably different and are given, together with data for the reactant, $U(NO_3)_4 \cdot 2$ L, compound A, in Table 1.

Evolved gas analysis (EGA) by gas chromatography (GC), with the Porapak column (see above) at 30°C gave the peaks shown in Fig. 4(a). During repeated sampling it was evident that a slower moving peak (or peaks) was bleeding off the column and disturbing the baseline. Increasing the column temperature to 110°C gave the sequence shown in Fig. 4(b). The elution

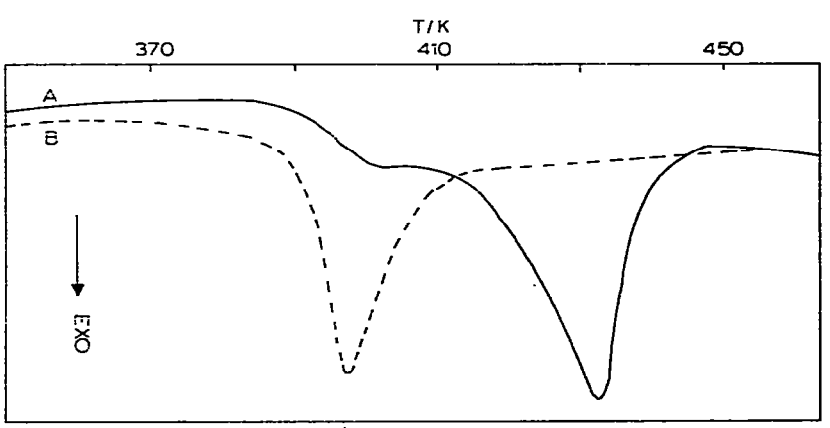

Fig. 3. DSC scans on $U(NO_3)_4 \cdot 2$ trispyrpo. Heating rate 5 K min^{-1} in He. A (———) ground <100 mesh, 6.75 mg; B (— — — —) crystal, 7.19 mg (N.B. sensitivity × 1/2).

TABLE 1

X-Ray powder diffraction data (CuK_α)

Compound A			Compound B			Compound C		
2θ	d (Å)	Rel. I (%)	2θ	d (Å)	Rel. I (%)	2θ	d (Å)	Rel. I (%)
9.76	9.054	37	9.54	9.263	68.5	10.30	8.581	37
10.40	8.499	100	11.04	8.007	100	18.95	4.677	100
15.46	5.726	37	11.20	7.843	100	24.36	3.651	48
20.18	4.396	21	18.56	4.776	52.5	25.90	3.429	33.5
			20.20	4.392	38.5	32.66	2.739	39

sequence given by Hollis and Wilhite [3] for Porapak Q at room temperature, with retention times relative to ethane (1.00), is N_2 (0.069), air (0.071), NO (0.080), N_2O (0.433) [with NO_2 only eluted on increasing the temperature and CO_2 (0.306) and H_2O (1.67)].

Peak 3 [Fig. 4(a)] was identified, by injection and by comparison with the products of NH_4NO_3 decomposition, as N_2O. Any NO formed would not be separated from any N_2 formed and the residual air peak (leak from the GSV), peak 1 on the trace. The observed increase in peak 1 above the background during decomposition (see Fig. 5) was not markedly suppressed when a liquid-air trap was interposed between the DSC and the GC. When the cold trap was removed, however, gas giving a peak in position 1 volatilized immediately. Peak 1 is thus a mixture of, at least, N_2 and NO. The gases giving peaks 2 and 3 were completely condensed by the cold trap.

At the higher column temperature (110°C), peaks 2 and 3 are not resolved and occur as a shoulder on peak 1 [see Fig. 4(b)]. The composite peak 4 + 5 is suggested to be mainly NO_2 accompanied by some H_2O. This peak is suppressed in the presence of the liquid-air trap. On allowing the trap to warm up, the gas volatilized much more slowly than NO, as expected for NO_2.

The presence of some H_2O in the decomposition products indicates that the stoichiometry is not as straightforward as suggested by eqn. (1) and that some oxidation of ligand by the evolved NO_2 is occurring. It is also suggested that peak 2 is CO_2 and that a contribution from CO could possibly be included in peak 1 (also non-condensable). The retention time for CO_2 (from injections and from the decomposition of nickel oxalate) is in agreement with that for peak 2. Ligand oxidation

$$L + NO_2 \rightarrow L' + N_2O + NO + N_2 + CO + CO_2 + H_2O \quad (2)$$

would also account for the presence of lower oxides of nitrogen and N_2, as well as the observed mass losses greater than calculated for reaction (1). The dissociated ligand is not sufficiently volatile to be detected in the EGA system.

Full profiles of gas evolution during scans on crystals at 5 K min^{-1} in He from 345 to 440 K (corrected) are shown in Fig. 5. The Porapak Q column was at 110°C for Fig. 5(a) and then reduced to 30°C for Figs. 5(b) and (c).

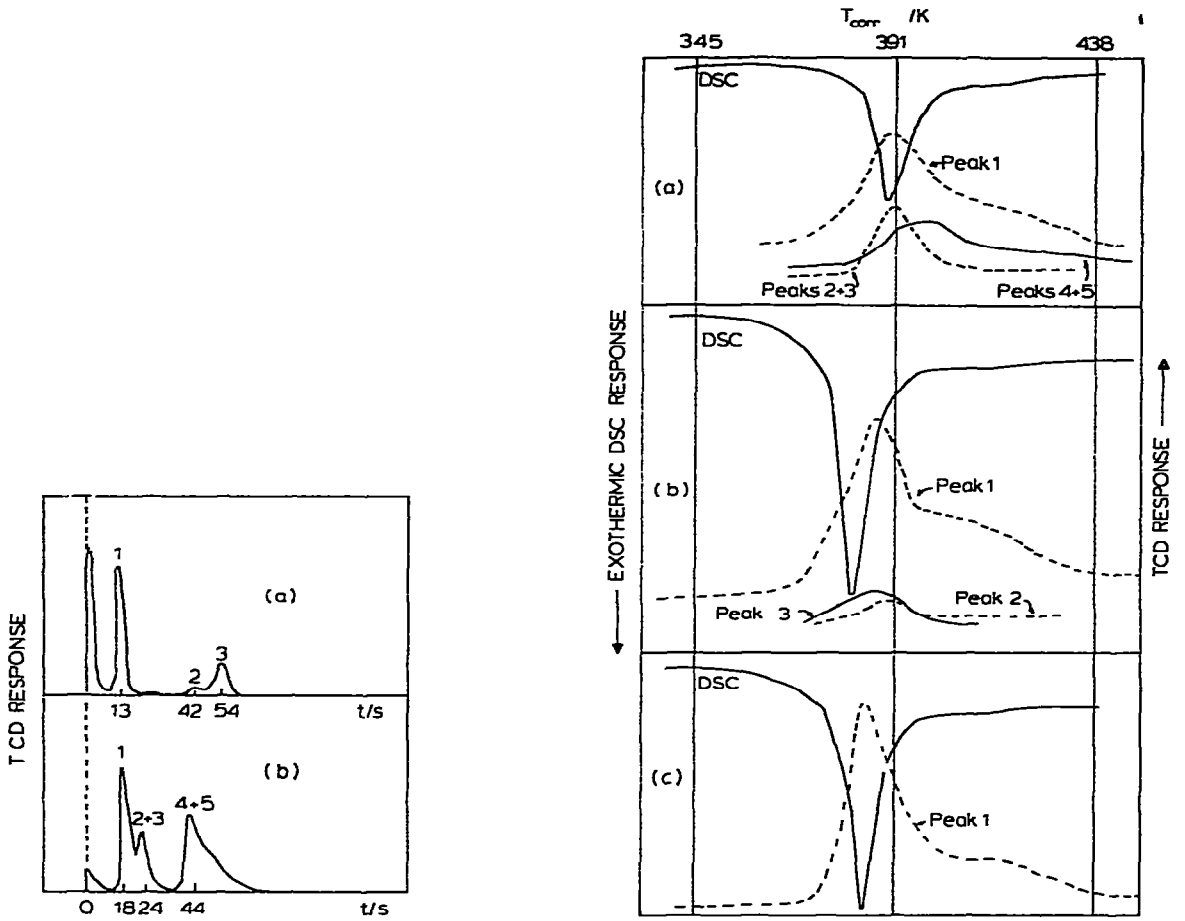

Fig. 4. GC response for single samplings of gases evolved in decomposition of $U(NO_3)_4 \cdot 2$ trispyrpo (He 5 cm^3 min^{-1}; chart 40 mm min^{-1}). (a) Porapak Q at 30°C; (b) Porapak Q at 110°C.

Fig. 5. DSC scans with EGA for the decomposition of crystals of $U(NO_3)_4 \cdot 2$ trispyrpo. Heating rate 5 K min^{-1} in He; Porapak Q column, He 5 cm^3 min^{-1}. (a) Column at 110°C, 7.19 mg sample; (b) column at 30°C, 13.00 mg sample; (c) column at 30°C, liquid-air trap interposed, 10.67 mg sample.

There are differences in the rates of evolution of the different gases which indicate changes in mechanism with temperature. Similar profiles for ground material (<100 mesh) are shown in Fig. 6. The change in the exothermic response brought about by grinding has already been noted. It is also possible that there is an ageing effect as the curves for freshly ground material (curves B and C) differed somewhat from that for 3-month old material (curve A).

Gas evolution profiles for an isothermal DSC run on crystals at 368 K (corrected) are shown in Fig. 7. At this temperature, decomposition of ground material was negligible. Evolution of all gases is at a maximum near the maximum of the exotherm, but peak 4 + 5 (i.e. NO_2 mainly) persists into the extended decay period. The reaction shown is accompanied by a mass

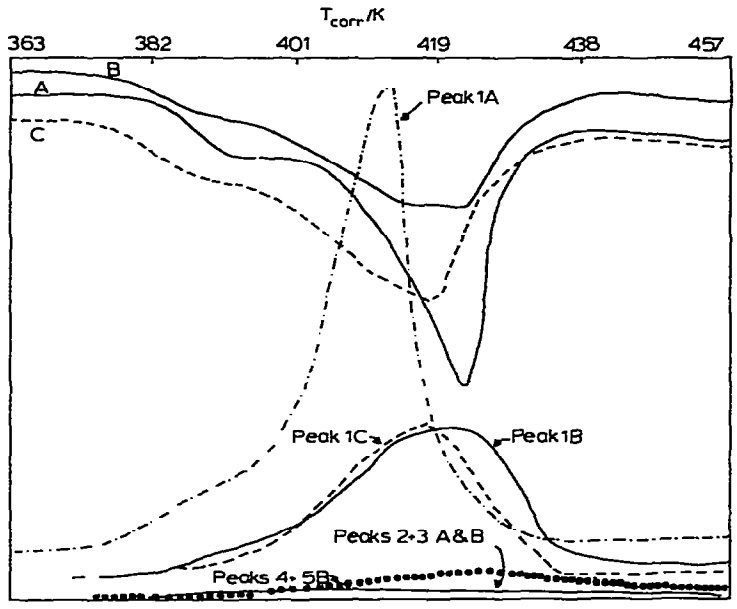

Fig. 6. DSC scans with EGA for the decomposition of ground (<100 mesh) $U(NO_3)_4 \cdot 2$ trispyrpo. Heating rate 5 K min^{-1} in He; Porapak Q column, He 5 cm^3 min^{-1}. A, 6.75 mg aged material, column at 30°C; B, 5.80 mg freshly ground, column at 110°C; C, 6.95 mg freshly ground, column at 110°C, liquid-air trap interposed.

loss of only 4.7% which could correspond either to a loss of only one NO_2 group per U atom, or to full decomposition, approximately according to reaction (1), at more reactive crystal zones. Only on further heating at higher temperatures does decomposition [reaction (1)] approach completion (>9.2% mass loss).

Kinetics from isothermal DSC runs

A series of isothermal DSC runs in helium, similar to that illustrated in Fig. 7, over the corrected temperature range 360—385 K, on crystals as prepared, gave mass losses ranging from 4.0 to 5.2%. The times to the maxima of the exotherms, t_{max} (see Fig. 7) were used to estimate approximate rate coefficients for reaction, $k_{ex} = 1/t_{max}$. These rate coefficients were then used in an Arrhenius plot to estimate the activation parameters for reaction. These were $E_a = 157 \pm 5$ kJ $mole^{-1}$ and $\ln (A/min^{-1}) = 49.1 \pm 1.7$. A similar series on the initial stage of the decomposition of ground material (<100 mesh), over the corrected temperature range 370—395 K, gave Arrhenius parameters $E_a = 185 \pm 14$ kJ $mole^{-1}$ and $\ln (A/min^{-1}) = 57.5 \pm 4.6$. This initial decomposition corresponds to a mass loss of the order of 1% compared to about 10% for the overall decomposition.

Kinetics from isothermal TG

Isothermal decomposition curves for crystals at temperatures from 358 to 370 K in N_2 are illustrated on two different time scales in Fig. 8(a) and (b).

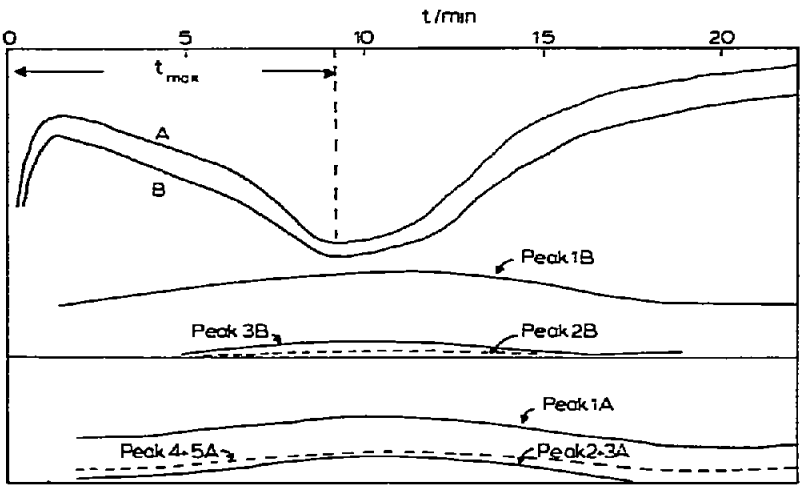

Fig. 7. Isothermal DSC scan with EGA for the decomposition of $U(NO_3)_4 \cdot 2$ trispyrpo crystals in helium at a corrected temperature of 368 K. Porapak Q column; He 5 cm^3 min^{-1}. A, 7.45 mg; column at 110°C; B 9.98 mg; column at 30°C.

An initially approximately linear region up to $\alpha \simeq 0.1$ is followed by a sigmoid section, leading into a very slow deceleratory period which only tends towards completion on the longer time scale of Fig. 8(b). There was some variation in behaviour of crystals grown at different rates. Arrhenius parameters were estimated from the temperature dependence of the slopes of the initial ($\alpha < 0.1$) linear regions of these curves as $E_a = 115 \pm 4$ kJ $mole^{-1}$ and $\ln (A/min^{-1}) = 33.7 \pm 1.4$, but the full curves were not amenable to detailed kinetic analysis.

On crushing the crystals to <200 mesh, the initial and sigmoid regions are eliminated and the overall decomposition rate is drastically reduced. This dramatic effect with decreasing particle size is illustrated in Fig. 9. The reaction which is now deceleratory throughout (Fig. 10) conforms approximately to the rate equation

$$(1-\alpha)^{-1/2} - 1 = kt$$

as shown in Figs. 10 and 11. From the linear plots in Fig. 11, E_a was estimated as 169 ± 17 kJ $mole^{-1}$ and $\ln (A/min^{-1})$ as 48.1 ± 5.4. These values compare fairly well with those obtained from isothermal DSC measurements.

The derivative form of the rate equation above is

$$\frac{d\alpha}{dt} = k'(1-\alpha)^{3/2}$$

which corresponds to an "index of reaction" [4] (superficially analogous to order of reaction) of $m = 3/2$ (z and $\beta = 1$). Taplin [4] has shown that powders with log-normal particle size distributions may exhibit such a high overall index of reaction even though the individual particles are decomposing according to the contracting volume ($m = 2/3$) or contracting area ($m = 1/2$) models [5]. As the decomposition kinetics have been shown to be very sensitive to particle size, no conclusion can be drawn about the geometrical

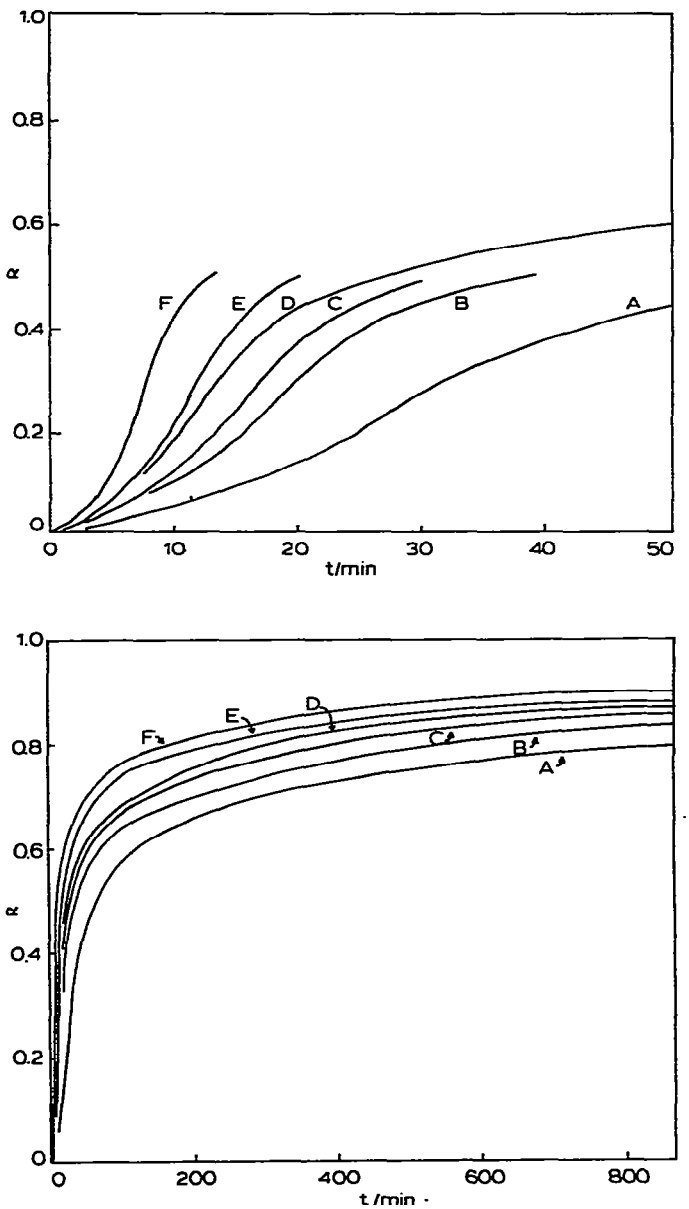

Fig. 8. Isothermal decomposition of crystals of $U(NO_3)_4 \cdot 2$ trispyrpo in nitrogen on short (a) and long (b) time scales. A, 358 K; B, 361.5 K; C, 363.5 K; D, 365 K; E, 366.5 K; F 370 K.

mechanism of decomposition of individual particles from the overall kinetics.

Thermochemistry

The areas under the exotherms (e.g. Fig. 3) were compared with the melting endotherm of pure indium metal ($\Delta H = 28.6_2$ J g^{-1}) and the enthalpy of

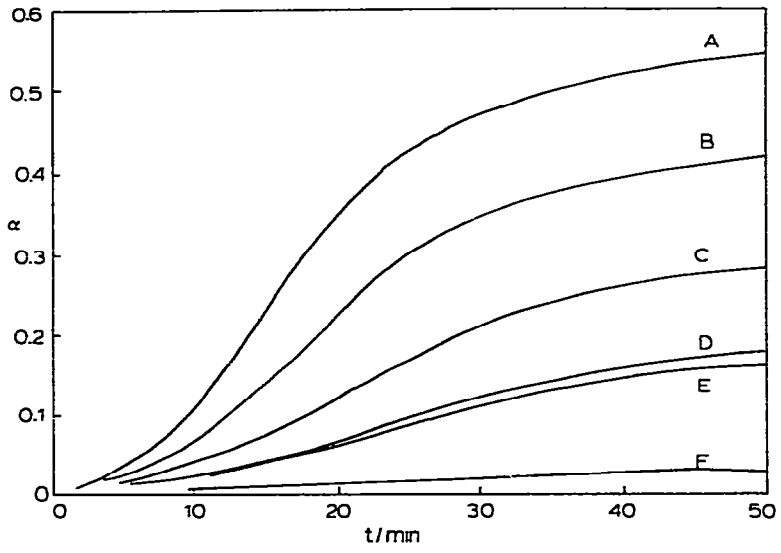

Fig. 9. Effect of particle size on the decomposition of $U(NO_3)_4 \cdot 2$ trispyrpo in nitrogen at 362 K. Mesh sizes: A, >30 mesh; B, 30—60 mesh; C, 60—100 mesh; D, 100—150 mesh; E, 150—200 mesh; F, <200 mesh.

decomposition of the crystals was estimated as -154 ± 4 kJ mole^{-1}. The value would contain contributions from both the reactions

$$U(NO_3)_4 \cdot 2\ L(s) \rightarrow UO_2(NO_3)_2 \cdot 2\ L(s) + 2\ NO_2(g) \quad (1)$$

and

$$L + NO_2 \rightarrow L' + N_2O + CO_2 + CO + NO \div N_2 + H_2O \quad (2)$$

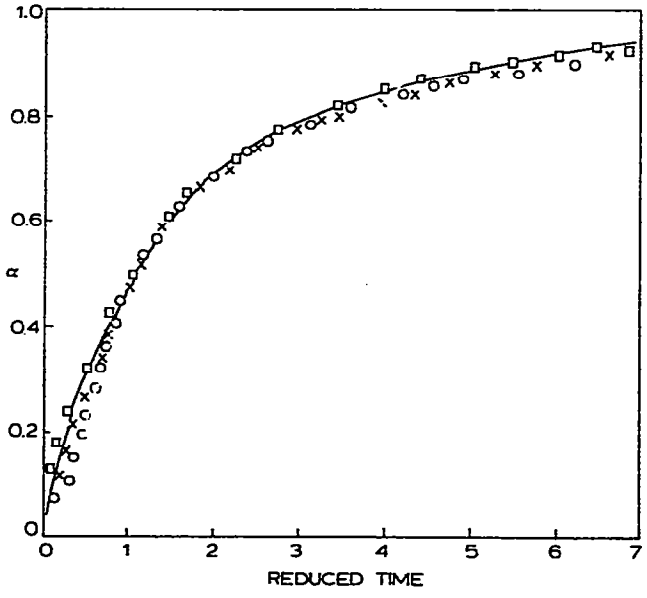

Fig. 10. Reduced-time plots for the decomposition of ground $U(NO_3)_4 \cdot 2$ trispyrpo in nitrogen. O = 375 K; X = 378 K; □ = 387 K. (———) Theoretical curve; $\alpha = 1 - (1 + kt)^{-2}$.

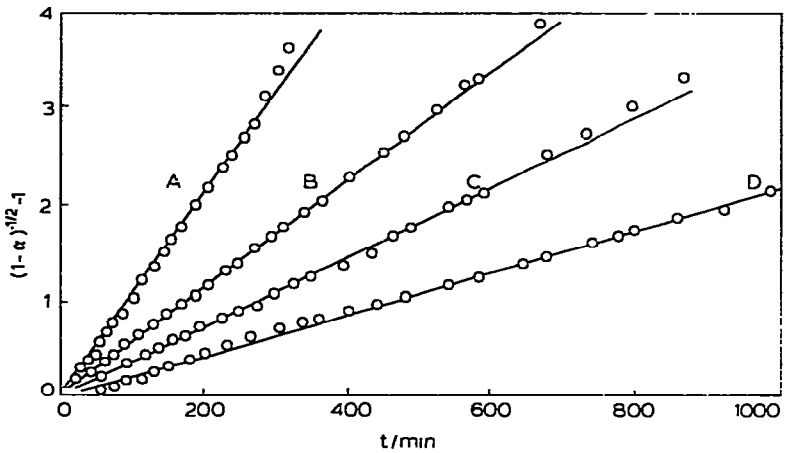

Fig. 11. Isothermal decomposition of ground (<200 mesh) $U(NO_3)_4 \cdot 2$ trispyrpo in nitrogen. Test of obedience to expression $(1-\alpha)^{-1/2} - 1 = kt$ A, 387 K; B, 383 K; C, 378 K; D, 375 K.

Lower values of ΔH were obtained for a few scans where oxidation was probably less extensive. The enthalpy of decomposition of ground (<100 mesh) $U(NO_3)_4 \cdot 2$ L was estimated, in a similar way to that for crystals, to be -108 ± 6 kJ mole^{-1}. This is low compared to the value for crystals (-154 ± 4 kJ mole^{-1}). It is suggested that less secondary oxidation [reaction (2)] occurs for ground reactant, from which escape of products, e.g. NO_2, is not impeded.

At relatively high heating rates, melting of the reactant accompanies decomposition and self-heating, caused by reaction (2) occurring in the melt, leads to explosive decomposition.

Hot-stage microscopy (HSM)

Crystals were found to be unstable under the high intensity illumination of the microscope. This photosensitivity is being studied further, but preliminary results show that there is a variation in sensitivity from crystal to crystal. At 30°C only a few crystals react. Reaction is within the crystal (confirmed by sectioning) and is accompanied by cracking. This cracking is sometimes, but not always, approximately parallel to cube faces and many of the fractures are conchoidal. Decomposition is definitely associated with the cracking as the brown colouration (NO_2?) begins in the cracked regions. Cracking is spasmodic, possibly due to critical pressures being achieved in gas pockets. Raising the temperature to 60°C did not cause any of the crystals (out of the light beam) to decompose thermally, but enhanced their sensitivity to photolysis.

CONCLUSIONS

Apparent activation energies for the decomposition of crystals increased with extent of decomposition, from 115 ± 4 kJ $mole^{-1}$ for the initial approximately linear region of the TG curves to 157 ± 5 kJ $mole^{-1}$ based on the DSC maxima. The apparent activation energies for ground material were higher, being 169 ± 17 kJ $mole^{-1}$ for the TG curves and 185 ± 14 kJ $mole^{-1}$ for the DSC maxima.

The measured enthalpies of decomposition were —154 ± 4 kJ $mole^{-1}$ for crystals, reducing to —108 ± 6 kJ $mole^{-1}$ for ground material. It is suggested that the main decomposition step for both crystals and ground material is reaction (1)

$$U(NO_3)_4 \cdot 2\,L(s) \rightarrow UO_2(NO_3)_2 \cdot 2\,L(s) + 2\,NO_2(g) \quad (1)$$

This reaction begins at defective regions on the surface and within the crystal. Within the crystal escape of $NO_2(g)$ is retarded and pockets of gas are formed. Within these pockets oxidation of ligand is possible [reaction (2)]

$$L + NO_2 \rightarrow L' + N_2O + NO + N_2 + CO + CO_2 + H_2O \quad (2)$$

This exothermic process both accelerates the rates of reactions (1) and (2) by self-heating and increases the gas pressure within pockets until cracking occurs. Unless precautions are taken, self-heating may be sufficient to cause melting. The cracking produces further defective regions. Once many channels have opened up for escape of the primary NO_2 product, very little secondary oxidation occurs and the completion of decomposition is relatively slow.

Crushing of reactant to a powder, which allows rapid escape of NO_2, greatly reduces the rate of decomposition, which becomes comparable with the final stages of decomposition of crystals, and also reduces the measured enthalpy of decomposition by lessening the extent of secondary reaction.

REFERENCES

1 J.G.H. du Preez, A. Litthauer and C.P.J. van Vuuren, Thermochim. Acta, 39 (1980) 163.
2 J.G.H. du Preez, A. Litthauer and C.P.J. van Vuuren, J. Therm. Anal., 19 (1980) 305.
3 L. Hollis and W.F.J. Wilhite, J. Gas Chromatogr., 6 (1980) 84.
4 J.H. Taplin, J. Am. Ceram. Soc., 57 (1974) 140.
5 M.E. Brown, D. Dollimore and A.K. Galwey, Comprehensive Chemical Kinetics, Vol. 22, Elsevier, Amsterdam, 1980.